

Fig. S1. XND-1 expression. Embryos and adult extruded germlines were stained with anti-XND-1 (red), anti-PGL-1 (white), and DAPI (green). Distal is to the left in all images. mit, mitotic zone; TZ, transition zone; P, pachytene; Dp, diplotene (A-A'') Anti-XND-1 antibodies do not stain *xnd-1* mutants. (A,A') *xnd-1*(-) embryos of indicated stage did not show XND-1 staining in PGC; non-specific background staining was seen in 550-cell stage embryos, most likely in the newly developed gut cavity. (A'') An *xnd-1*(-) adult germ line did not show XND-1 staining, demonstrating the specificity of anti-XND-1 antibody (Also see Wagner et al., 2010) (B) XND-1 staining was readily seen in the wild-type germ line.

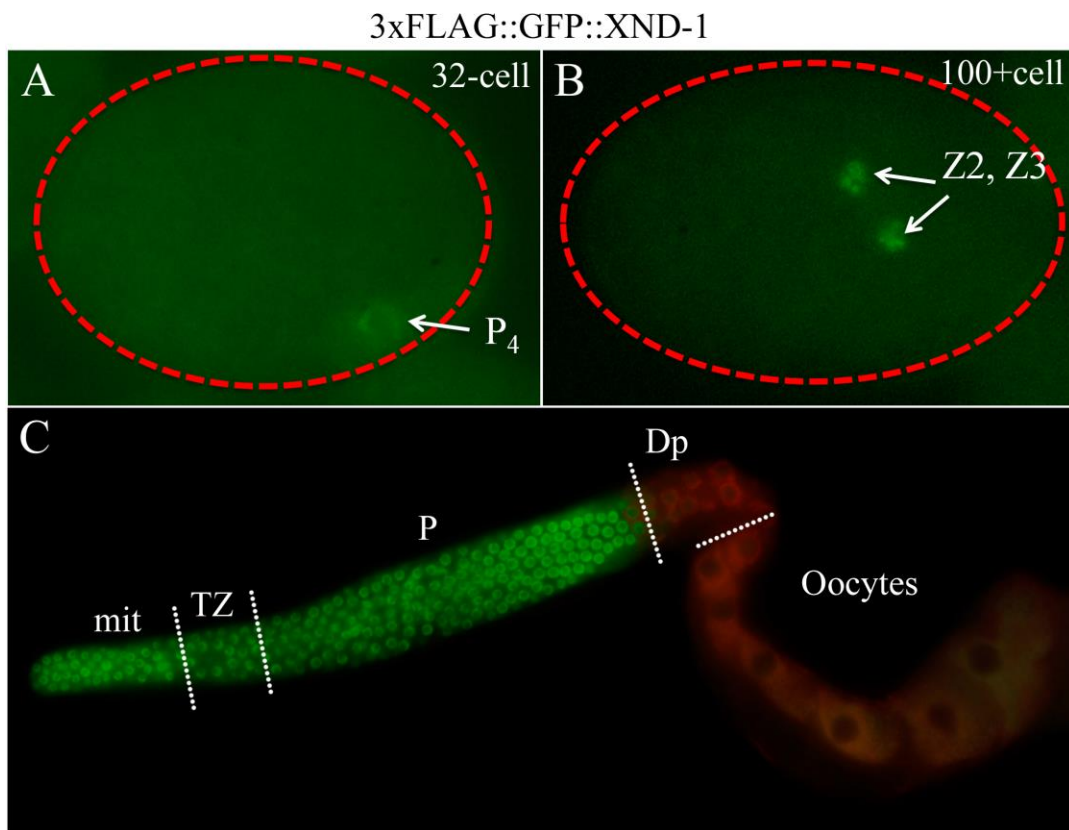


Fig. S2. XND-1 expression using a 3xFLAG::GFP-tagged *xnd-1* transgene. Embryos are oriented anterior to the left and outlined with red dotted line; in adult germ lines, distal is toward the left. (A-C) 3xFLAG::GFP::XND-1 (green) was expressed in the *xnd-1*(-) background. (C) Red color in the proximal adult germ line is the autofluorescence recorded by the color camera. GFP fluorescence is absent in the proximal region. mit, mitotic zone; TZ, transition zone; P, pachytene; Dp, diplotene.

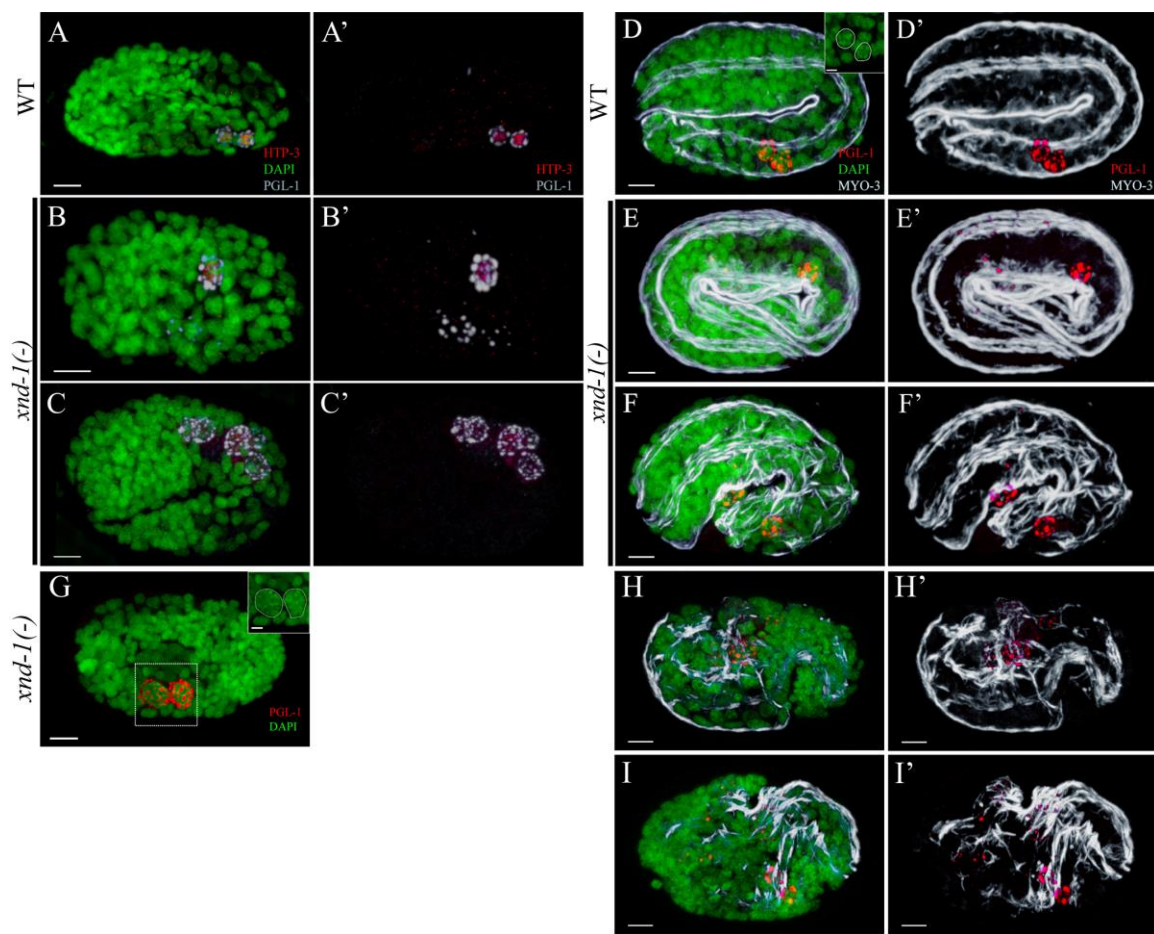


Fig. S3. *xnd-1*(-) embryos exhibit PGCs defects. All embryos are oriented anterior to the left. (A-C) >200+ cell embryos of indicated genotypes stained with anti-PGL-1 to mark P-granules (white), anti-HTP-3 to mark PGCs (red) and DAPI to mark nuclei (green). HTP-3/DAPI/PGL-1 (A-C), HTP-3 /PGL-1 (A'-C'). (B) Blastomeres with missegregated P-granules do not show HTP-3 staining. (C) Embryo with four PGCs showing both PGL-1 and HTP-3. (D-F,H,I) 550-cell embryos of indicated genotypes stained with anti-PGL-1 to mark PGCs (red), anti-MYO-3 (mAB5-6) to mark muscle cells (white), and DAPI to mark nuclei (green). PGL-1/ DAPI /MYO-3(D-F), PGL-1/MYO-3 (D'-F'). (D) Wild type. (E) Misseggregated PGL-1 is found in muscle cells. (F) Aberrant muscle morphology and mislocalized PGCs can frequently be observed together. (G) *xnd-1* embryo showing enlarged PGCs (inset) compared to the PGCs of wild type in (D) (inset) . (H,I) *xnd-1* embryos showing aberrant muscle morphology. Scale bar: 5 μm for all embryos and 2 μm for all insets.

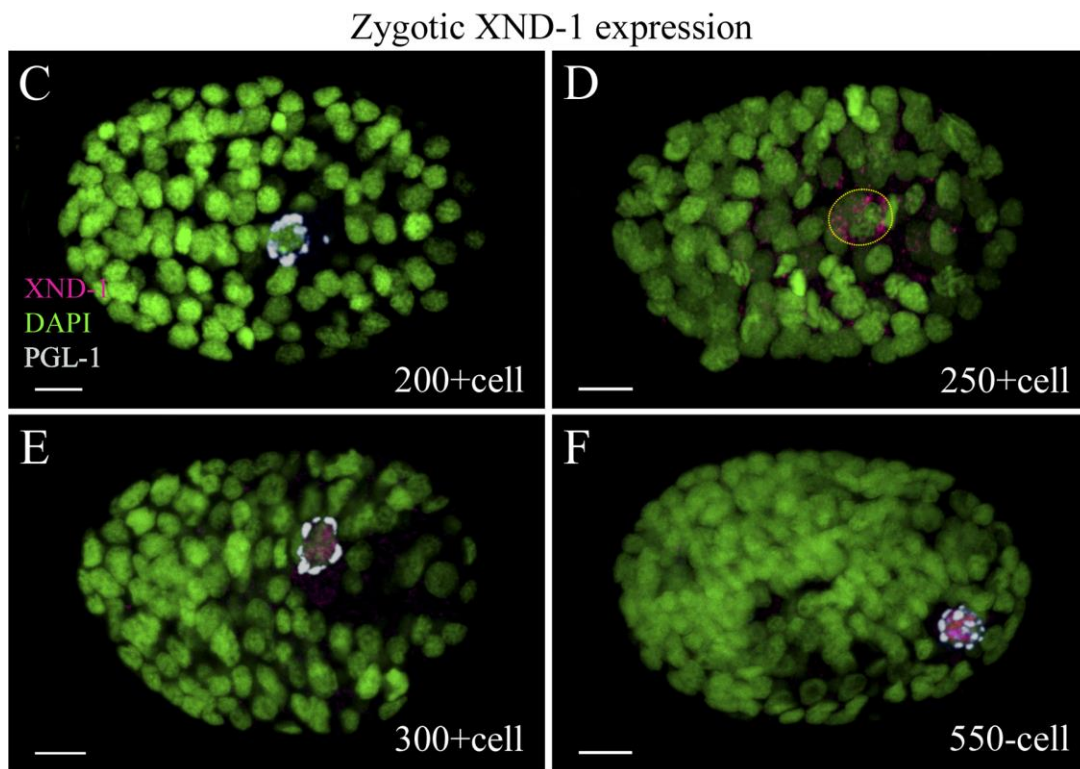
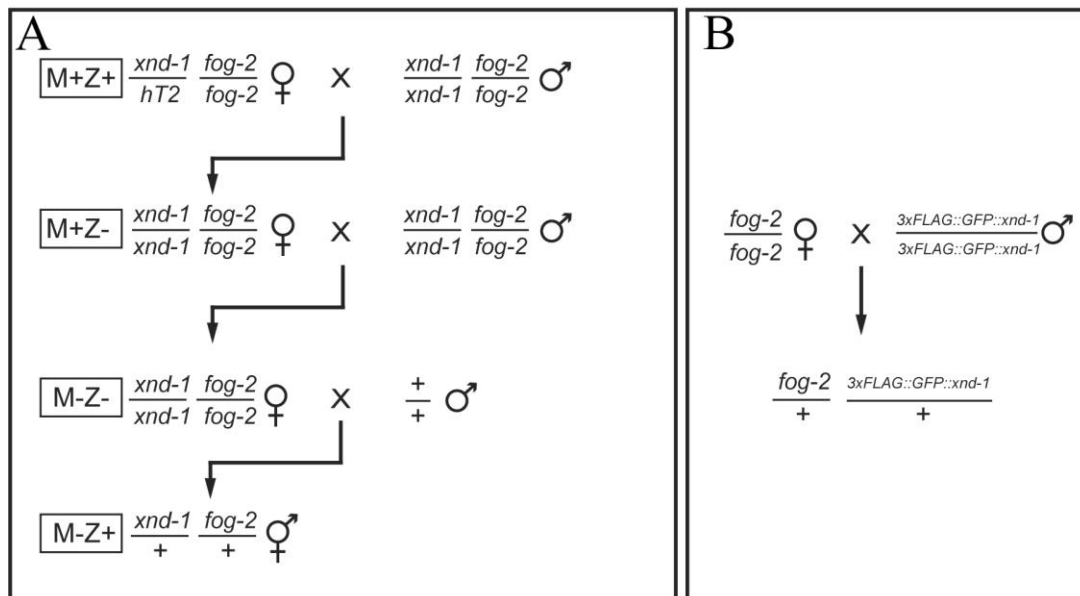


Fig. S4 (A,B) Schematics of genetic crosses used to generate *xnd-1* M+Z-, *xnd-1* M-Z- and *xnd-1* M-Z+ animals for analysis. (B) Genetic cross to get *3xFLAG::GFP::xnd-1* transgene in WT background. (C-F) *xnd-1* M-Z+ embryos, despite expressing XND-1, exhibited PGCs defects. (D-F) Embryos showed one large PGC.

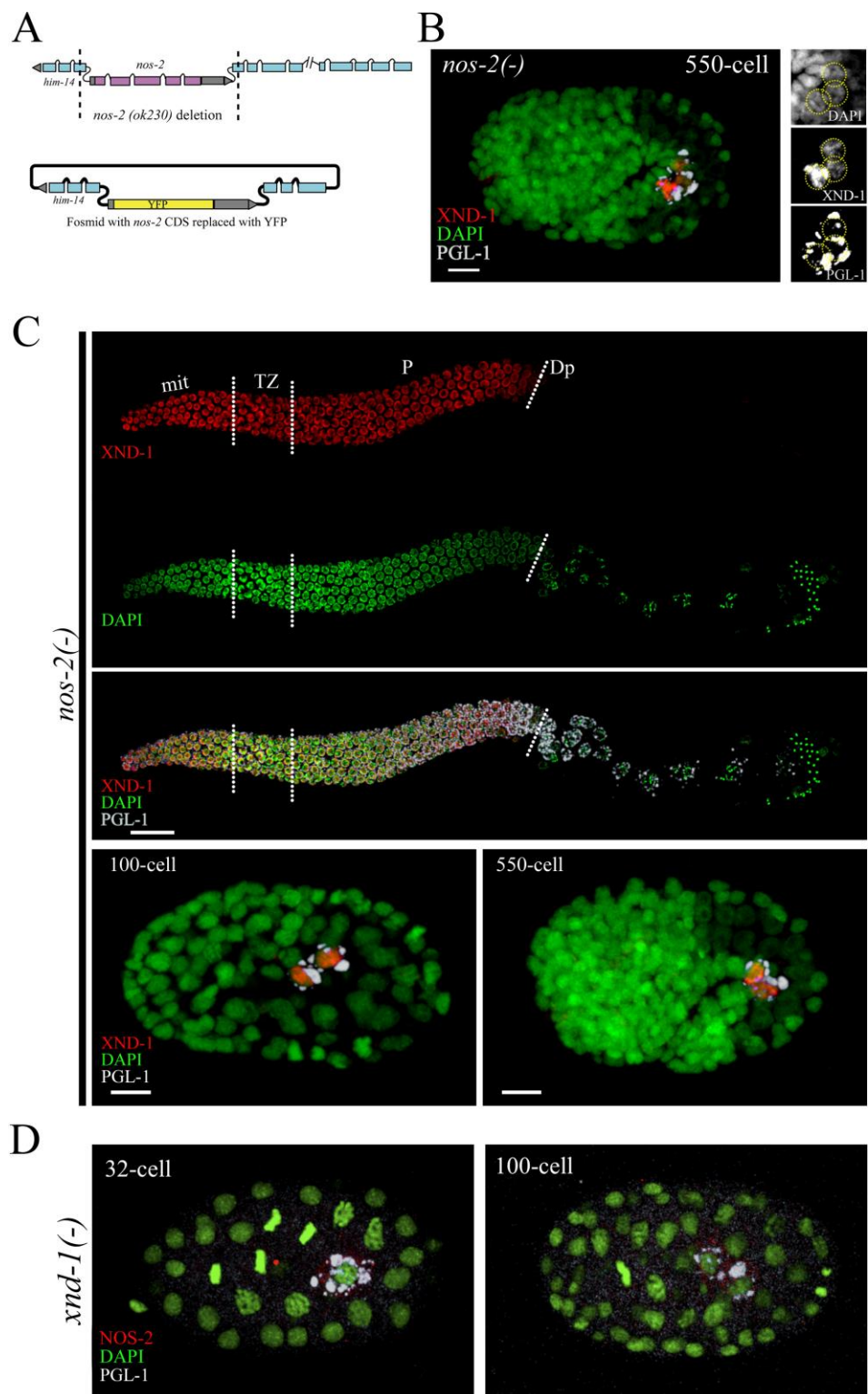


Fig. S5. (A) Schematic of the *nos-2* (*ok230*) deletion. Top: Illustration shows the portion of *him-14* gene containing *nos-2*. Boxes represent exons and wavy lines represent introns. The deletion in the *ok230* allele is marked with dotted lines. Bottom: Schematic of the

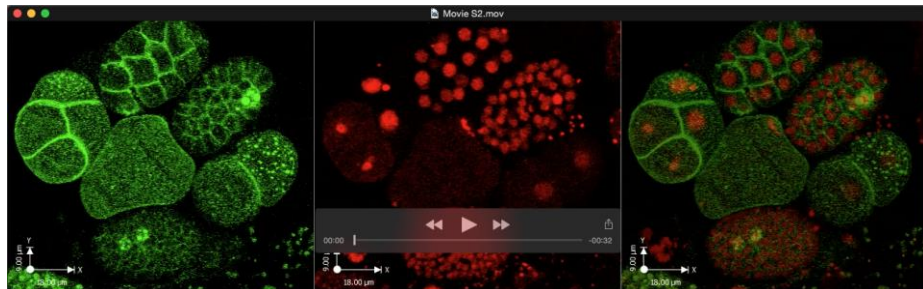
fosmid used to create the *nos-2*(-) animals in which the *nos-2* coding sequence is replaced with YFP. (B,C) Embryos and adult germ lines of *nos-2* mutants are stained with anti-XND-1 (red), anti-PGL-1 (white) and DAPI (green). All embryos are oriented anterior to the left, and extruded germ lines are oriented distal to the left. mit, mitotic zone; TZ, transition zone; P, pachytene; Dp, diplotene (B) A representative 550-cell stage embryo showing premature proliferation of PGCs. Inset shows the PGCs with respective staining. (C) Adult germ lines and embryos showing normal expression of XND-1 identical to that of wild type. (D) *xnd-1*(-) embryos of indicated cell stages stained with anti-PGL-1 (white), anti-NOS-2 (red) and DAPI (green). Scale bar: 5 µm for embryos and 20 µm for germline.



Movie 1. Available at link:

<https://www.dropbox.com/s/88xvsu8vzyjy2zo/Movie%20S1.mov?dl=0>

P₄ division in wild-type embryos. Left panel: PGL-1::GFP (Green) to mark germ line lineage and GFP::PH(PLC1delta1) (Green) to mark cell membranes; middle panel: mCherry::H2B (red) to mark the nuclei; right panel: merged. Six embryos can be seen in different developmental stages and P₄ cell divide in all of them.



Movie 2. Available at link:

<https://www.dropbox.com/s/6l6nlblskaq1ljx/Movie%20S2.MOV?dl=0>

P₄ failed to divide in *xnd-1*(-) embryos. Left panel: PGL-1::GFP (Green) to mark germ line lineage and GFP::PH(PLC1delta1) (Green) to mark cell membranes; middle panel: mCherry::H2B (red) to mark the nuclei; right panel: merged. Five embryos can be seen in different developmental stages and P₄ cell did not divide in the top and lower right embryos in the film.

Table S1. 3xFLAG::GFP::*xnd-1* transgene rescues *xnd-1*(-) brood and embryonic lethality

Strain	Genotypes	% Hatching	% Embryonic lethality	Total laid eggs ± SD	N
<i>xnd-1</i> (-)	<i>unc-119 xnd-1; xnIs273</i> [fJN059: <i>him-14</i> with <i>nos-2</i> replaced by <i>yfp</i> , <i>unc-119</i> (+) line 25]	14	86	45±22.5	10
Control	<i>unc-119; eaIs6</i> [3xflag::gfp::sbp:: <i>xnd-1</i> + <i>unc-119</i> (+) transgene]	98	2	168±22.5	10
<i>xnd-1</i> (-); <i>eaIs6</i>	<i>unc-119 xnd-1; eaIs6</i> [3xflag::gfp::sbp:: <i>xnd-1</i> + <i>unc-119</i> (+) transgene]	94	6	162±45.2	10

This analysis was done at 25°C

Table S2. *xnd-1* and *nos-2* animals are sterile and lack germ lines

Strain	Genotype	% Sterile adults	% lack of germ lines	N
	Wild type	0	0	557
<i>xnd-1(-)</i>	<i>xnd-1(-); xnIs273</i> 20°C	13 (295)*	3	927
<i>nos-1(-)</i>	<i>unc-119 xnd-1/hT2; nos-1(gv5): xnIs273</i> 20°C	1.4	N.D.	442
<i>nos-1(-); xnd-1(-)</i>	<i>unc-119 xnd-1; nos-1(gv5); xnIs273</i> F2 Adults at 20°C	16	1.5	340
<i>nos-2(-)</i>	<i>unc-4 nos-2 (ok230); xnIs273</i> 20°C	3.4	1	1492
<i>nos-2(-)</i>	<i>unc-4 nos-2 (ok230); xnIs273</i> 25°C	8 (1095)*	7	1653
<i>nos-2(-)</i>	<i>unc-119 xnd-1/hT2; nos-2 (ok230); xnIs273</i> 20°C	4.4	1.7	408
<i>nos-2(-); xnd-1(-)</i>	<i>unc-119 xnd-1; nos-2 (ok230); xnIs273</i> F2 Adults at 20°C	57	24	486
<i>nos-1(-); nos-2(-)</i>	<i>nos-1 nos-2; xnIs273</i> 20°C	51	47.5	645
<i>nos-1(-); nos-2(-)</i>	<i>nos-1 nos-2; xnIs273</i> 25°C	47	43	1324
<i>nos-1(-); nos-2(-)</i>	<i>nos-1 (gv5) nos-2 (ok230); xnIs273</i> F2 Adults at 20°C	48	45	770
<i>nos-1(-); nos-2(-)</i>	<i>unc-119 xnd-1/hT2; nos-1 (gv5) nos-2 (ok230); xnIs273</i> F2 Adults at 20°C	54	44	755
<i>nos-1(-); nos-2(-); xnd-1(-)</i>	<i>unc-119 xnd-1; nos-1 (gv5) nos-2 (ok230); xnIs273</i> F2 Adults at 20°C	98	92	553

*Independent quantification of sterility was performed, so N values are shown in brackets and final column represents the number of animals tested for no germ line. N.D. not determined.

Table S3. Modified *him-14* fosmid uncovers the function of *nos-2*

Strain	% Hatching	% Embryonic lethality	Total laid eggs ± SD	N
<i>him-14 nos-2(ok230)</i>	2	98	207.5± 24.2	9
<i>nos-2(-)*</i>	98.2	1.8	204.5± 55.6	10
<i>nos-1(-) nos-2(-)*</i>	95	5	166± 53.5	11

Analysis was done at 20°C.

* *nos-2(-):unc-4(e120) nos-2 (ok230)II; xnIs273 [fJN059: him-14 with nos-2 replaced by yfp, unc-119(+)]*

Table S4. H3K4me2 is upregulated in PGCs of *xnd-1* and *nos-2*; *xnd-1* embryos

H3K4me2 staining in PGCs in >200-cell embryos								
Genotypes	% One PGC embryos			% Two PGCs embryos			Total % embryos with H3K4me2 positive PGCs	N
	Unstained	Stained	N	Unstained	One stained	Both stained		
WT 20°C				80.5	11.5	8	19.5	190
<i>nos-2(-) 20°C</i>				87.5	4.5	8	12.5	224
<i>xnd-1(-) 20°C</i>	45	55	247	64.5	7.5	28	47	160
<i>nos-2(-); xnd-1(-) 20°C</i>	18	82	147	27.5	13	59.5	77	138
<i>nos-1(-) nos-2(-) 25°C</i>				17	23	60	83	117

PGCs were identified as PGL-1 positive and were examined for the co-staining of H3K4me2. One and two PGC embryos were examined from the same slides but counted in two separate categories.

Table S5. List of *C. elegans* strain used in this study

Strain Name	Genotype	Transgene	Reference
CB4108	<i>fog-2(q71) V</i>		CGC
DP132	<i>edIs6 (IV)</i>	<i>edIs6 [unc-119::GFP + rol-6(su1006)] IV</i>	CGC
OH439	<i>otIs118</i>	<i>otIs118 [unc-33::GFP + unc-4(+)]</i>	CGC
QP391	<i>xnd-1(ok709)III/ hT2[bli-4(e937) let-?(q782) qIs48] (I;III)</i>		(Wagner et al., 2010)
QP432	<i>him-5(ok1896) V</i>		(Meneely et al., 2012)
QP770	<i>xnd-1(ok709)III/ hT2[bli-4(e937) let-?(q782) qIs48] (I;III); bnIs1; ltIs37; ItIs38</i>	<i>bnIs1[pie-1::GFP::pgl-1 + unc-119(+)] I. ltIs37 [pAA64; pie-1::mCherry::HIS-58 + unc-119(+)] IV. ltIs38 [pAA1; pie-1::GFP::PH(PLC1delta1) + unc-119(+)].</i>	This Study
QP837	<i>xnd-1(ok709)III/ hT2[bli-4(e937) let-?(q782) qIs48] (I;III); fog-2(q71)V</i>		This Study
QP922	<i>unc-119(ed3) xnd-1(ok709)III; eaIs6</i>	<i>eaIs6[3xFLAG::GFP::SBP::xnd-1+unc-119(+) transgene]</i>	This Study
QP954	<i>unc-119(ed3) xnd-1(ok709)III; hT2[bli-4(e937) let-?(q782) qIs48] (I;III); unc-4(e120) nos-2 (ok230)II; xnIs273</i>	<i>xnIs273 [fJN059: him-14 with nos-2 replaced by yfp, unc-119(+) line 25].</i>	This Study
QP956	<i>unc-4(e120) nos-2 (ok230)II; xnIs273</i>		This Study
QP957	<i>unc-119(ed3) xnd-1(ok709)III; hT2[bli-4(e937) let-?(q782) qIs48] (I;III); xnIs273</i>		This Study
QP974	<i>nos-2 (ok230) nos-1(gv5)/mC6[GFP] II; xnIs273</i>		This Study
QP1018	<i>nos-1(gv5); unc-119 xnd-1(ok709)III/ hT2[bli-4(e937) let-?(q782) qIs48] (I;III); xnIs273</i>		This Study
QP1019	<i>nos-2(ok230); unc-119 xnd-1(ok709)III/ hT2[bli-4(e937) let-?(q782) qIs48] (I;III); xnIs273</i>		This Study
QP1020	<i>nos-2(ok230)nos-1(gv5); unc-119 xnd-1(ok709)III/ hT2[bli-4(e937) let-?(q782) qIs48] (I;III); xnIs273</i>		This Study
QP1143	<i>xnd-1(ok709)III/ hT2[bli-4(e937) let-?(q782) qIs48] (I;III); edIs6(IV)</i>	<i>edIs6 [unc-119::GFP + rol-6(su1006)] IV</i>	This Study
QP1144	<i>xnd-1(ok709)III/ hT2[bli-4(e937) let-?(q782) qIs48] (I;III); otIs118</i>	<i>otIs118 [unc-33::GFP + unc-4(+)]</i>	This Study

Supplementary materials and methods

Constructing *nos-2*(-) strain

Primers (*yfp* coding sequences in caps):

5' gaaaataaacgggttggacccgatataaaaaagtattgagaaattggatcttcta TTTGTATAGTTCATCCAT
GCCATG

galK was removed by arabinose-induced expression of FLP recombinase, and the fosmid region containing *him-14* was subcloned into pCJF151, which contains the *unc-119(+)* gene (Frokjaer-Jensen et al., 2008). Subcloning was performed by gap repair and selection on LB plates containing chloramphenicol + ampicillin.

Primers (pCFJ151 sequence in caps):

5' cttatctttcaaaaacaagttgtcgagtcaatttttttcagaCGTATTATAAGTGCAAGTAAGA
TCAGTG

5' cacaaggatataatccatttctatcgagccaccaggtagttatGGCCTAGTTCTAGACATTCTCT
AATG

Immunostaining

For staining, two-day old adults were mounted in M9 and dissected to release embryos that were fixed in 1% paraformaldehyde for 5 min and snap frozen on slides on a pre-frozen metal block on dry ice. Samples were freeze-cracked to permeabilize and placed in -20°C methanol for 1 min, then post-fixed with 2% paraformaldehyde for 15 min at room temperature. Samples were blocked with 0.1% bovine serum albumin with 1X phosphate buffered saline containing 0.1% Triton X-100 (PBST). Samples were hybridized overnight in primary antibody, washed 3 x 10 min in PBST then hybridized at room temperature for at least two hours in secondary antibody. Washes were performed 3 x 10 min in PBST with DAPI added to the second wash. Samples were mounted on slides with ProLong Gold antifading agent (Molecular Probes Cat# P36935) and hardened overnight prior to imaging.

Antibodies were used at the following concentrations: rabbit anti-PGL-1 1:30000 (Kawasaki et al., 1998); mouse monoclonal mAb K76 1:10 (DSHB)(Strome and Wood,

1982); mouse anti-FLAG M2 1:500 (Sigma Aldrich # F1804); guinea pig anti-XND-1 1:2000 (Wagner et al., 2010); rabbit anti-NOS-2 1:40 (Subramaniam and Seydoux, 1999); rabbit PhosphoDetect™ anti-Cdk1 (pTyr¹⁵) 1:100 (Calbiochem, # 219440); rabbit anti-dimethyl-Histone H3 (Lys4) 1:1000 (Upstate # 07-030); mouse monoclonal mAb 5-6 (anti-MYO-3) 1:20 (DSHB) (Miller et al., 1983); mouse monoclonal mAb F2F4 (anti-Cyclin B) 1:50 (DSHB)(Shakes et al., 2009).

The following secondary antibodies were used at a concentration of 1:1000: Donkey anti-Rabbit IgG (H+L) Alexa Fluor® 488 (Novex#:A-21206); Goat anti-Rabbit IgG (H+L)Alexa Fluor® 568 (Novex#:A-11011); Goat anti-Guinea Pig IgG (H+L) Alexa Fluor® 568 (Novex#:A-11075); Goat anti-Guinea Pig IgG (H+L) Alexa Fluor® 488 (Novex#:A-11073); Goat anti-Mouse IgG (H+L) Alexa Fluor® 568 (Novex#:A-11004); Goat anti-Mouse IgG (H+L) Alexa Fluor®488 (Novex#:A-11001).

- Frokjaer-Jensen, C., Davis, M. W., Hopkins, C. E., Newman, B. J., Thummel, J. M., Olesen, S. P., Grunnet, M. and Jorgensen, E. M.** (2008). Single-copy insertion of transgenes in *Caenorhabditis elegans*. *Nature genetics* **40**, 1375-1383.
- Kawasaki, I., Shim, Y.-H., Kirchner, J., Kaminker, J., Wood, W. B. and Strome, S.** (1998). PGL-1, a Predicted RNA-Binding Component of Germ Granules, Is Essential for Fertility in *C. elegans*. *Cell* **94**, 635-645.
- Miller, D. M., Ortiz, I., Berliner, G. C. and Epstein, H. F.** (1983). Differential localization of two myosins within nematode thick filaments. *Cell* **34**, 477-490.
- Shakes, D. C., Wu, J. C., Sadler, P. L., Laprade, K., Moore, L. L., Noritake, A. and Chu, D. S.** (2009). Spermatogenesis-specific features of the meiotic program in *Caenorhabditis elegans*. *PLoS genetics* **5**, e1000611.
- Strome, S. and Wood, W. B.** (1982). Immunofluorescence visualization of germ-line-specific cytoplasmic granules in embryos, larvae, and adults of *Caenorhabditis elegans*. *Proc Natl Acad Sci U S A* **79**, 1558-1562.
- Subramaniam, K. and Seydoux, G.** (1999). nos-1 and nos-2, two genes related to *Drosophila nanos*, regulate primordial germ cell development and survival in *Caenorhabditis elegans*. *Development (Cambridge, England)* **126**, 4861-4871.
- Wagner, C. R., Kuervers, L., Baillie, D. L. and Yanowitz, J. L.** (2010). xnd-1 regulates the global recombination landscape in *Caenorhabditis elegans*. *Nature* **467**, 839-843.